

Local magnetovolume effects in Fe₆₅Ni₃₅ alloys

F. Liot and I. A. Abrikosov

Department of Physics, Chemistry, and Biology (IFM), Linköping University, SE-581 83 Linköping, Sweden

(Received 15 July 2008; revised manuscript received 5 November 2008; published 8 January 2009)

A systematic *ab initio* study of static ionic displacements in a face-centered-cubic Fe₆₅Ni₃₅ alloy has been carried out. Theoretical results for magnitudes of average Fe-Fe, Fe-Ni, and Ni-Ni $\langle 110 \rangle$ bond vectors agree well with experimental measurements. In addition, we have observed that in collinear ferrimagnetic states, iron-iron nearest-neighbor pairs with antiparallel local magnetic moments are shorter on average than those with parallel moments. Furthermore, having considered different states (ferromagnetic, nonmagnetic, and collinear ferrimagnetic states) for the same lattice spacing, we have shown that the magnetic structure strongly influences local geometrical properties of the alloy. For example, a transition from a ferromagnetic state to a collinear ferrimagnetic state induces a significant contraction of the volume associated with an iron site where the moment flips. A model system based on a Hamiltonian written as the sum of Lennard-Jones energies and a classical Heisenberg Hamiltonian has been introduced. It yields structural properties which are qualitatively similar to those obtained *ab initio*. We have found that some of the phenomena can be classified as magnetovolume effects.

DOI: [10.1103/PhysRevB.79.014202](https://doi.org/10.1103/PhysRevB.79.014202)

PACS number(s): 75.30.-m, 75.50.Bb

I. INTRODUCTION

Invar Fe₆₅Ni₃₅ alloy is one of the most fascinating magnetic materials. Toward the end of the 19th century, Guillaume¹ discovered that a face-centered cubic (fcc) iron-nickel alloy with 35 at. % Ni exhibited a very small thermal-expansion coefficient (less than $1.2 \times 10^{-6} \text{ K}^{-1}$ at room temperature) in a wide temperature interval. Following the publication of Guillaume's original paper, a vast amount of experimental data concerning the Invar alloy was collected.² It revealed the existence of other anomalous physical properties such as a downward deviation of the ideal lattice constant from the value predicted by Vegard's law, a departure of the saturation magnetic moment from the Slater-Pauling curve, and an unusual temperature dependence of the magnetization.

Although the origin of the Invar effect has been extensively theoretically investigated, it is still controversial. It is clear that there is a negative contribution to the thermal-expansion coefficient which compensates at some temperature the positive contribution coming from the anharmonicity of the lattice vibrations.³ Moreover, it is generally believed that the former contribution is related to magnetic properties of the alloy. However, there is no consensus on the nature of this relationship. In the *latent antiferromagnetism* model, the anomalous expansion arises from an increasing number of pairs of antiparallel local magnetic moments (LMMs) on increasing temperature.⁴ On the other hand, according to Shiga⁵ as well as Yamada and Nakai,⁶ it is due to a decrease of the magnitudes of the LMMs. In addition, Weiss⁷ demonstrated that the thermal excitation from a high-moment large-volume ferromagnetic state to a low-moment small-volume antiferromagnetic state can give rise to the anomaly.

With the present paper, we wish to contribute to a better understanding of the dependence of local structure in Invar Fe₆₅Ni₃₅ alloy on local magnetic arrangement. Besides two of the models mentioned above, various previous works suggest the existence of a correlation between the local magnetic

moment at an Fe site and a corresponding local volume.^{8,9} In particular, the model proposed in Ref. 8 relies on the assumption of local volume expansion with increasing local moment and accounts for Invar properties of fcc iron-nickel alloys. Furthermore, Krauss and Krey⁹ reported that the volume for an atom in amorphous iron at zero temperature tends to be larger for larger LMM. However, to the best of our knowledge, previous *ab initio* calculations carried out for Fe-Ni Invar alloys neglected the existence of static ionic displacements in this system. In this work we study the effect systematically and focus on the relations between local structural and local magnetic properties in the alloy.

This article is organized as follows. In Sec. II, computational details of the first-principles calculations are given. Results of structural properties of the alloy are presented in Sec. III. To gain insight into the origin of some of the effects described in Sec. III, a model is proposed in Sec. IV. Section V is devoted to the summary.

II. COMPUTATIONAL METHODS

We apply the "special quasirandom structures" (SQSs) method¹⁰ to random fcc Fe₆₅Ni₃₅ alloy. We choose this approach because it has already been successfully utilized to investigate local lattice relaxations in transition-metal alloys.^{11,12} SQSs are relatively small-unit-cell periodic structures designed so that the Warren-Cowley short-range-order parameters (α 's) are as close to zero as possible for the relevant coordination shells.¹³ In the case of random fcc Fe₆₅Ni₃₅ alloy, earlier works on chemical and magnetic interactions indicate that the α 's should be as close to zero as possible up to the fourth shell.^{14,15} We take into account this recommendation and generate an SQS using a technique described in Ref. 16. The final structure has an Fe atomic concentration of 64.58% (62 Fe atoms and 34 Ni atoms per supercell) and is such that the number of like atoms in the first coordination shell of an Fe atom varies from 4 to 11.

All calculations are carried out by the Vienna *ab initio*

simulation package (VASP).^{17,18} The projector augmented wave (PAW) method is chosen.¹⁹ The cutoff energy for the plane-wave basis set is 267.91 eV. Integrals over the first Brillouin zone are approximated by weighted sums over special \mathbf{k} points determined according to the Monkhorst-Pack scheme.²⁰ The generalized-gradient approximation (GGA) in the Perdew-Wang 1991 form (PW91) is employed for the exchange-correlation energy functional.²¹ We remark here that it is not clear if the GGA gives more accurate description of magnetic properties of transition-metal alloys as compared to the local-density approximation (LDA).^{13,22} However, contrary to LDA calculations, GGA computations correctly predict the ground state of Fe to be ferromagnetic and body-centered cubic.^{23,24} Moreover, equilibrium atomic volumes of $3d$ metals calculated within the GGA are known to be in better agreement with experimental results. Because in this work we carry out full structural optimization of the ionic positions in our SQS and we are particularly interested in the effect of static ionic displacement the use of the GGA is justified.

At a given volume and for a given initial magnetic configuration, a structural relaxation is performed under the constraints that neither the shape nor the volume of a supercell changes until the magnitude of the force acting on each atom is smaller than approximately $0.020 \text{ eV}/\text{\AA}$. Afterwards, using the linear tetrahedron method with Blöchl corrections as well as a $5 \times 5 \times 5$ Monkhorst-Pack grid, the total energy for the relaxed structure is converged to less than $0.01 \text{ meV}/\text{atom}$. Although the LMMs are allowed to fluctuate during the calculations, none of them changes sign.

Here, we discuss the set of initial configurations for the self-consistent spin-polarized computations. It is well known that GGA calculations predict that the alloy at equilibrium is ferromagnetic (FM).^{15,22} For this reason, we include a FM configuration in the set. Also, we plan to characterize the change of the local structure around an iron site due to the flip of the local magnetic moment at the site. It appears that a collinear ferrimagnetic (CF) structure with a local moment at an iron site surrounded by the largest number of iron neighboring atoms which is antiferromagnetically aligned with the magnetization is particularly suitable for such a study. Indeed, this structure is predicted to be the magnetic configuration which is the energetically closest to the ferromagnetic state of the alloy around the equilibrium volume.²²

III. FIRST-PRINCIPLES RESULTS

We begin the presentation of our first-principles data with a description of equilibrium magnetic properties of the alloy. As can be deduced from Fig. 1, the most stable state is found to be ferromagnetic. Although this conclusion agrees well with the result of other recent numerical works,^{15,22} it seems to contradict some experimental evidences that in Invar $\text{Fe}_{65}\text{Ni}_{35}$ at low temperature, the magnetic structure consists in a few percent of local magnetic moments that are oriented antiparallel to the magnetization.²⁵ The discrepancy most probably originates from the use of the GGA. In particular, several earlier LDA calculations predicted the stability of ferrimagnetic states at theoretical and/or experimental

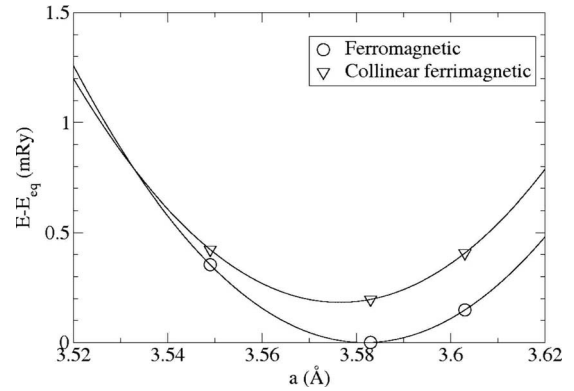


FIG. 1. Total energies per atom (relative to the equilibrium value) of $\text{Fe}_{65}\text{Ni}_{35}$ alloy in various states as functions of the lattice constant according to *ab initio* calculations. Circles: data for ferromagnetic states. Triangles: data for collinear ferrimagnetic states. Continuous lines: fits to parabolic functions.

volumes.^{15,26–28} Unfortunately, they also strongly underestimated the alloy lattice parameter, which makes it problematic to using the LDA for the present study. Moreover, in Ref. 22 it was emphasized that though it is perhaps impossible to predict exactly the magnetic ground state of Fe and Fe-based alloys with the present day level of first-principles calculations based on the local exchange-correlation functionals, one can still study the trends in the alloy systems, e.g., the magnetovolume effect, which is the main subject of this work.

Concerning the magnetic properties of the alloy in the theoretical ground state, the average magnetic moment of an iron atom is estimated to be $2.53\mu_B$, while Ni moments average to $0.65\mu_B$. More information about the distribution of the individual quantities is given below. For the net moment, the discrepancy between our computational value ($1.86\mu_B/\text{atom}$) and an experimental observation ($1.75\mu_B/\text{atom}$) can be attributed to the above-mentioned underestimation of the fraction of moments which are anti-aligned with the total moment.

We now report on structural properties of the system at equilibrium. It should be noted that the calculated lattice spacing is 3.583 \AA , within 0.2% of an experimental result.²⁹

In random fcc Fe-Ni alloy with 35 at. % Ni, atoms lying in dissimilar low-symmetry environments (e.g., one Fe coordinated by a $\text{Fe}_{11}\text{Ni}_1$ cluster and another Fe coordinated by Fe_7Ni_5) have *a priori* distinct nonzero static displacements (see Fig. 2). As a result, the alloy might manifest a distribution of $\langle 110 \rangle$ bond vectors and a distribution of first neighbor spacings. In this paper, we write the average bond vector of an Fe-Fe $\langle 110 \rangle$ pair as $\|\langle \mathbf{R}_{ij}^{\text{eq}} \rangle_{\text{FeFe}}^{110}\|$. We use the corresponding notations for Fe-Ni and Ni-Ni pairs ($\|\langle \mathbf{R}_{ij}^{\text{eq}} \rangle_{\text{FeNi}}^{110}\|$ and $\|\langle \mathbf{R}_{ij}^{\text{eq}} \rangle_{\text{NiNi}}^{110}\|$). The calculated distances are displayed in Fig. 3, relative to the mean separation between two first neighbors d^{NN} . d^{NN} is equal to $a/\sqrt{2}$, where a denotes the lattice constant. As expected from the foregoing discussion, the magnitudes of the average bond vectors differ from each other and from d^{NN} . In addition, as can be observed in Fig. 3, the predicted values compare qualitatively well with the experimental results of Robertson *et al.*³⁰ obtained at 60 K from

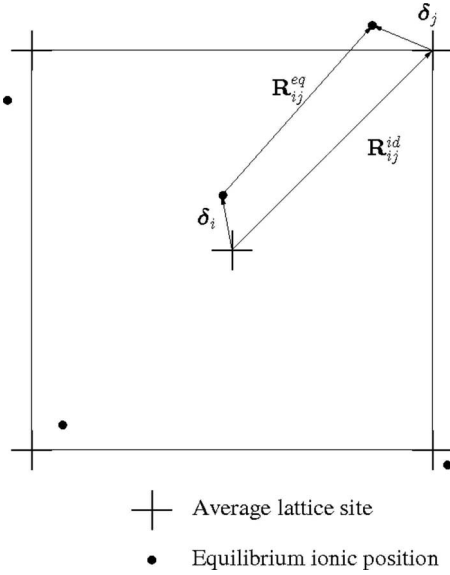


FIG. 2. Average lattice sites and equilibrium ionic positions in a substitutional alloy at equilibrium represented schematically. Note that the bond vector of the ionic pair (i, j) is displaced by $\delta_j - \delta_i$ from the average lattice vector \mathbf{R}_{ij}^d .

diffuse x-ray scattering methods. This is particularly remarkable since the lattice distortions are small (less than 0.020 \AA) on average.

The mean Fe-Fe, Fe-Ni, and Ni-Ni nearest-neighbor bond lengths are reported in Fig. 4(a). Clearly, the three distances $d_{\text{FeFe}}^{\text{NN}}$, $d_{\text{FeNi}}^{\text{NN}}$, and $d_{\text{NiNi}}^{\text{NN}}$ all lie away from d^{NN} . Even so, the weighted average of the spacings, $(1-x)^2 d_{\text{FeFe}}^{\text{NN}} + 2(1-x)x d_{\text{FeNi}}^{\text{NN}} + x^2 d_{\text{NiNi}}^{\text{NN}}$, follows the average first neighbor bond length.³¹ Moreover, the Fe-Ni separation is the shortest. This assertion is obviously in contradiction with an intermediate distance predicted by the hard-sphere model (see e.g., Refs. 32 and 33). At this stage, we would like to stress that the discrepancy between $d_{\text{FeFe}}^{\text{NN}}$ and $\|\langle \mathbf{R}_{ij}^{\text{eq}} \rangle_{\text{FeFe}}^{110}\|$ is significant (0.007 \AA) and thus recommend not to confuse the average Fe-Fe nearest-neighbor (NN) distance with the magnitude of the mean Fe-Fe $\langle 110 \rangle$ bond vector. In an effort to

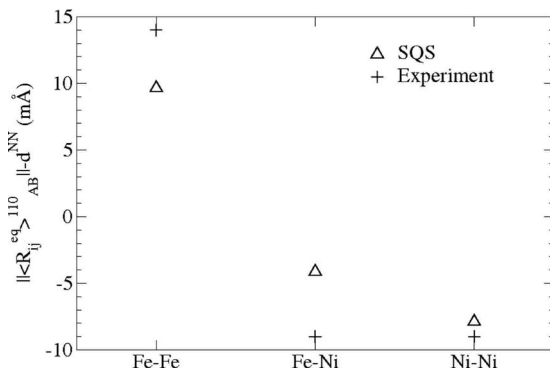


FIG. 3. Magnitudes of average Fe-Fe, Fe-Ni, and Ni-Ni $\langle 110 \rangle$ bond vectors (relative to the mean distance between first neighbors). Triangles: *ab initio* results for $\text{Fe}_{65}\text{Ni}_{35}$ alloy in the lowest energy ferromagnetic state. Crosses: experimental results for $\text{Fe}_{63}\text{Ni}_{37}$ alloy at 60 K (Ref. 30).

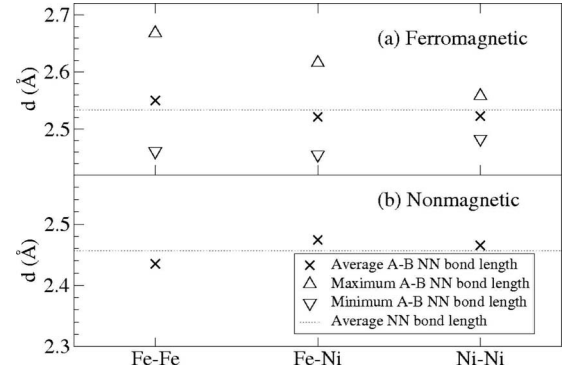


FIG. 4. Characteristics of the distributions of Fe-Fe, Fe-Ni, and Ni-Ni nearest-neighbor bond lengths in $\text{Fe}_{65}\text{Ni}_{35}$ alloy in various states, according to *ab initio* calculations. (a) Data for the lowest energy ferromagnetic state. (b) Data for the lowest energy nonmagnetic state.

gain understanding in the mechanism responsible for the relative order of $d_{\text{FeFe}}^{\text{NN}}$, $d_{\text{FeNi}}^{\text{NN}}$, and $d_{\text{NiNi}}^{\text{NN}}$, we give in Fig. 4(b) the calculated mean spacing between two Fe-Fe, Fe-Ni, and Ni-Ni first neighbors in the lowest energy nonmagnetic state. Surprisingly, the Fe-Fe distance is considerably lowered as the magnetic configuration changes from FM to NM. For an analysis of this behavior, please refer to Sec. IV.

Regarding distributions of interatomic distances in $\text{Fe}_{65}\text{Ni}_{35}$ at equilibrium, Fig. 4(a) indicates that the longest bond is 9% longer than the shortest one. Therefore, individual static displacements can be quite large.

It is also interesting to investigate the dependence of the mean distance between two sites on the relative orientation of the two moments. Figure 5 displays the calculated average separation of a pair of first neighbor iron sites in collinear ferrimagnetic $\text{Fe}_{65}\text{Ni}_{35}$ alloy for each relative orientation (parallel and antiparallel) of the two moments. Clearly, ferromagnetic Fe-Fe NN pairs are longer on average than antiferromagnetic ones. We provide an explanation for this behavior in Sec. IV. Let us now put our findings into perspective. Experiments have shown that fcc $\text{Fe}_{65}\text{Ni}_{35}$ alloy at low temperature exhibits a collinear ferrimagnetic

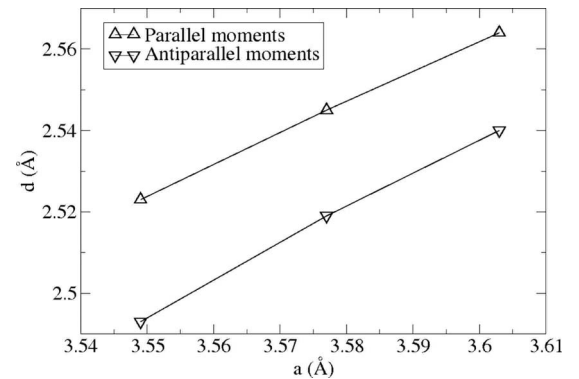


FIG. 5. Average Fe-Fe nearest-neighbor bond lengths in collinear ferrimagnetic $\text{Fe}_{65}\text{Ni}_{35}$ alloy as functions of the lattice constant according to *ab initio* calculations. The Fe-Fe pairs are distinguished on the relative orientation of their moments: parallel (triangles up) or antiparallel (triangles down).

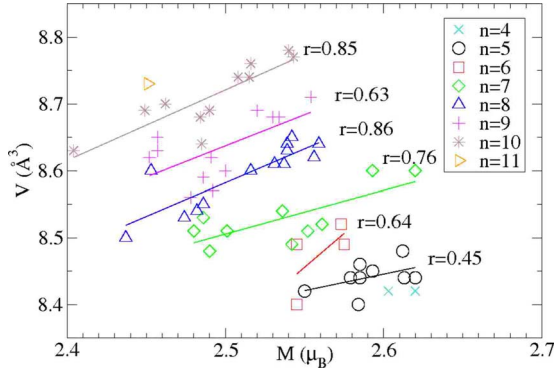


FIG. 6. (Color online) Local volumes of Fe atoms in ferromagnetic $\text{Fe}_{65}\text{Ni}_{35}$ alloy with $a=3.583 \text{ \AA}$ versus local magnetic moments according to *ab initio* calculations. For each n between 5 and 10, the regression line shows that the volume of an atom surrounded by n like first neighbors tends to expand with increasing moment.

structure²⁵ and a lattice constant that deviates from Vegard’s law.³⁴ Although it is still unclear how the fraction of antiparallel Fe-Fe NN pairs is related to the deviation, the following mechanism can be imagined: as the fraction increases from zero, the average distance between first neighbor iron sites contracts. This contraction in turn leads to a shrinkage of the average bond length.

We now turn our attention to the main purpose of this paper, namely, the investigation of how fluctuations in the magnetic arrangement affect local geometrical properties of $\text{Fe}_{65}\text{Ni}_{35}$. In contrast to earlier works,^{9,35} we define the volume associated with each iron site (volume of each Fe atom) in terms of the mean distance between the site and its first neighbors. The correlation between the local magnetic moment and the volume of an Fe atom is presented in Figs. 6 and 7 for the ferromagnetic and collinear ferrimagnetic states with $a=3.583 \text{ \AA}$.

Note that earlier first-principles calculations showed that for Fe-Ni alloys net magnetic moments, as well as average magnetic local moments at Fe atoms, decreased with decreasing volume.^{15,27,36,37} Quite unexpectedly, we see no apparent LMM-volume correlation, i.e., local magnetovolume effect, over the whole set of Fe sites in $\text{Fe}_{65}\text{Ni}_{35}$ in the ferromagnetic state. However, if we restrict ourselves to the set

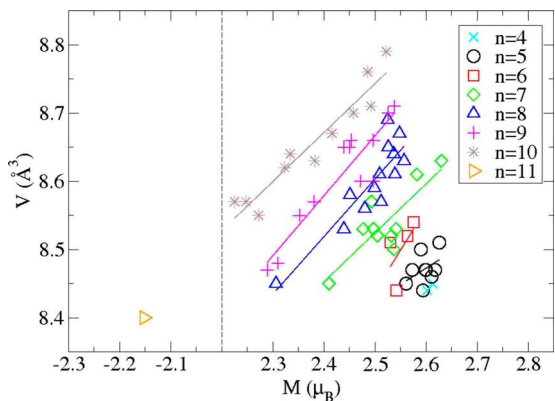


FIG. 7. (Color online) As in Fig. 6, but in collinear ferrimagnetic $\text{Fe}_{65}\text{Ni}_{35}$ alloy with $a=3.583 \text{ \AA}$.

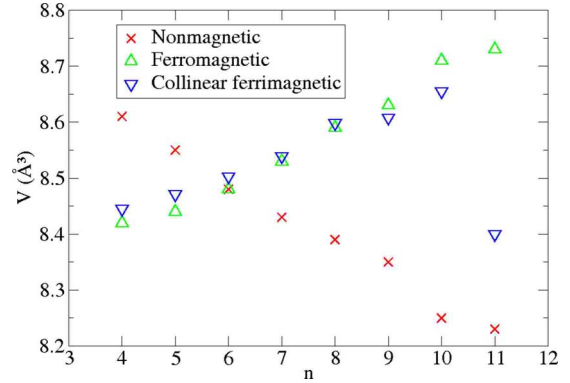


FIG. 8. (Color online) The average local volume of an Fe atom coordinated with n like nearest neighbors as a function of n , according to first-principles calculations. Crosses, triangles up, and triangles down: results for the nonmagnetic, ferromagnetic, and collinear ferrimagnetic states with $a=3.583 \text{ \AA}$.

of iron atoms with FM moments and placed in a similar environment (with the same number of like NNs), we actually obtain a positive correlation coefficient r . Hence, the corresponding regression line indicates that a contraction of local volume tends to accompany a local moment decrease.

Figure 7 reveals another prominent structural feature of the alloy in the CF state. The volume of an atom with a moment oriented antiparallel to the magnetization (8.40 \AA^3) is reduced with respect to that of any atom with an aligned moment. Also, it is 4% smaller than the volume of the same atom in the FM state (8.73 \AA^3). This unusual effect seems particularly noteworthy in light of the *latent antiferromagnetism* model⁴ mentioned in Sec. I.

To explore the influence of the local environment on the local geometry, we evaluate numerically the average volume of an iron atom coordinated with n like atoms for several values of n and for various states (NM, FM, and CF states with $a=3.583 \text{ \AA}$). The calculated quantities are shown in Fig. 8. We observe that different states exhibit a different dependence of the mean volume on the parameter characterizing the local environment. Indeed, while the volume shrinks with increasing n in the NM state, it expands up to $n=10$ in the two other states. Nevertheless, in contrast to the FM state, the CF state shows a nonmonotonic behavior since $V_{11} < V_{10}$. The reader interested in the origin of this phenomenon is referred to Sec. IV.

IV. MODEL RESULTS AND PHYSICAL EXPLANATIONS

Within the proposed model, the Hamiltonian H for $\text{Fe}_{65}\text{Ni}_{35}$ alloy has the following form:

$$H = \sum_{\langle ij \rangle} E_{ij}, \quad (1)$$

where $E_{ij}(d_{ij}, \mathbf{e}_i, \mathbf{e}_j)$ is the interaction energy between site i and site j , d_{ij} is an intersite distance, and \mathbf{e}_i is a unit vector oriented in the direction of the moment at site i . The sum runs over all pairs of nearest neighbors. For each of these pairs, the interaction energy is expressed as

$$E_{ij}(d_{ij}, \mathbf{e}_i, \mathbf{e}_j) = E_{ij}^{\text{LJ}}(d_{ij}) - J_{ij}(d_{ij}) \mathbf{e}_i \cdot \mathbf{e}_j, \quad (2)$$

where $E_{ij}^{\text{LJ}}(d_{ij})$ is the chemical (nonmagnetic) part of the interaction energy and $J_{ij}(d_{ij})$ is an exchange interaction energy between the LMMS at sites i and j . As in Refs. 38 and 39, the former is taken to be of the Lennard-Jones type

$$E_{ij}^{\text{LJ}}(d_{ij}) = -E_{ij}^0 \left[2 \left(\frac{d_{ij}^0}{d_{ij}} \right)^6 - \left(\frac{d_{ij}^0}{d_{ij}} \right)^{12} \right]. \quad (3)$$

d_{ij}^0 and E_{ij}^0 are two parameters which characterize E_{ij}^{LJ} . Following earlier works,^{14,40,41} we model the magnetic part of the energy by a classical Heisenberg Hamiltonian. Note that model Hamiltonians combining the LJ model with some Ising model have already been used to study the relation between anomalous magnetovolume behavior and magnetic frustration in Invar alloys³⁸ and perform Monte Carlo simulation of magnetovolume effects in Fe-Ni alloys.³⁹ Here we apply the Hamiltonian H to understand our *ab initio* results concerning the relations between magnetic and geometrical properties of Fe₆₅Ni₃₅.

As a matter of fact, we are particularly interested in studying structural properties of the model in the following states: (i) the lowest energy nonmagnetic state (the NM state), (ii) the lowest energy ferromagnetic state (the FM state), and (iii) the lowest energy state in which the only iron site which is surrounded by 11 like nearest neighbors exhibits a moment oriented antiparallel to the magnetization, whereas the moment at any other site is parallel (the CF state). It is worth emphasizing here that we are primarily concerned with qualitative features of structures, as well as providing simple explanations of observed phenomena.

As a preliminary step, we determine the distance d_{ij}^+ that minimizes the interaction energy E_{ij} (the equilibrium distance) of an Fe-Fe first neighbor pair (i, j) for miscellaneous magnetic configurations. We make the following choices for the parameters of the energy E_{ij} . E_{ij}^0 and d_{ij}^0 are assigned the value of 11 mRy and 2.435 Å, respectively. Note that d_{ij}^0 is chosen equal to our *ab initio* result of the average iron-iron first neighbor bond length in the lowest energy nonmagnetic state [see Fig. 4(b)]. Regarding the exchange parameter for the ferromagnetic ($\mathbf{e}_i \cdot \mathbf{e}_j = 1$) and antiferromagnetic ($\mathbf{e}_i \cdot \mathbf{e}_j = -1$) configurations, the curve of J_{ij} in the interval between 2.4 and 2.6 Å is plotted in Fig. 9(b). J_{ij} exhibits a well-known behavior.^{14,39} It is negative at 2.45 Å, positive at 2.55 Å, possesses a local minimum in between, and varies slowly from 2.58 to 2.6 Å. The calculated equilibrium distances are presented in Table I. We observe that d_{ij}^+ is larger for the ferromagnetic configuration than for the antiferromagnetic (AFM) one, while the nonmagnetic arrangement yields the smallest separation. Figure 9 provides further insight into the physics underlying these findings. It actually displays the curve of E_{ij}^{LJ} , $-J_{ij} \mathbf{e}_i \cdot \mathbf{e}_j$, and E_{ij} for the FM and AFM configurations. Obviously, the dependence of the equilibrium spacing d_{ij}^+ on the scalar product between the vectors \mathbf{e}_i and \mathbf{e}_j arises from the dependence of the exchange coupling J_{ij} on the intersite distance.

Next, we compare the calculated mean iron-iron nearest-neighbor bond length in the NM state to the one in the FM state. The former (latter) distance is approximated as the

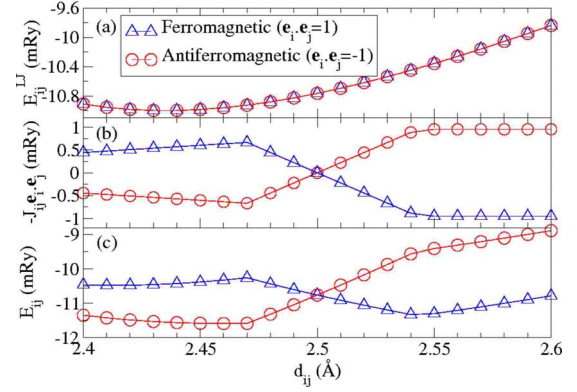


FIG. 9. (Color online) Triangles: (a) The Lennard-Jones, (b) the exchange, and (c) the interaction energies of a ferromagnetic pair of first neighbor iron sites as functions of the intersite distance according to our model. Circles: As above, but for an antiferromagnetic pair.

equilibrium separation d_{ij}^+ of an Fe-Fe first neighbor pair (i, j) for the NM (FM) arrangement. In the case of the NM state, as expected from the choice of d_{ij}^0 ($d_{ij}^0 = 2.435$ Å), the model prediction for the average Fe-Fe first neighbor bond length is in perfect agreement with the corresponding *ab initio* data of 2.435 Å, shown in Fig. 4(b). However, the most significant model result concerns the difference between the average separation in the FM state and the one in the NM state: it is close to the corresponding first-principles value of 0.115 Å. An important conclusion is drawn at this stage. The discrepancy may be a magnetovolume effect.

Then, we calculate the average separation of a pair of first neighbor iron sites for each relative orientation (parallel and antiparallel) of the two moments in the CF state. The former (latter) distance is approximated as the equilibrium separation d_{ij}^+ of an Fe-Fe first neighbor pair (i, j) for the FM (AFM) arrangement. In agreement with our first-principles result, we find that the antiparallel Fe-Fe NN pairs are shorter on average than the parallel ones. This phenomenon clearly originates from the variation of J_{ij} with the intersite spacing.

Pursuing the investigation of structural properties of the model, we turn to the dependence of the average local volume of an iron atom surrounded by 12 nearest neighbors on the number of like atoms in the first coordination shell. First, we define the volume of an iron atom i coordinated by a Fe _{n} Ni_{12- n} cluster as $4/3 \times \pi \times r_i^3$, where r_i is equal to half of

TABLE I. The equilibrium distance of an Fe-Fe first neighbor pair (i, j) for several magnetic arrangements according to our model. The distance for the ferromagnetic ($\mathbf{e}_i \cdot \mathbf{e}_j = 1$) and antiferromagnetic ($\mathbf{e}_i \cdot \mathbf{e}_j = -1$) configuration has been determined from Fig. 9(c).

Type of configuration	d_{ij}^+ (Å)
Nonmagnetic	2.435
Ferromagnetic	2.543
Antiferromagnetic	2.466

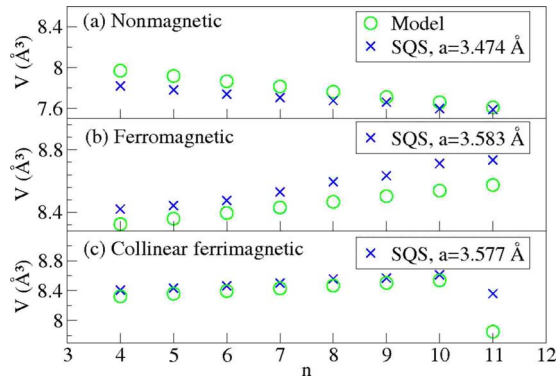


FIG. 10. (Color online) The average local volume of an iron atom in $\text{Fe}_{65}\text{Ni}_{35}$ in (a) nonmagnetic, (b) ferromagnetic, and (c) collinear ferrimagnetic states versus the number of iron atoms in the first coordination shell. Circles: model results. Crosses: *ab initio* results.

the distance (in Å) of $[\sum_j d_{ij}^+ + (12-n) \times 2.5]/12$. In the above expression, the sum runs over the Fe NNs. Note that the volume v_i is best understood as the volume of the atom i in the case that all the bonds with its Fe neighbors are energetically satisfied, and the distance from atom i to every Ni NN is 2.5 Å. The last mentioned value is chosen intermediate between the average Fe-Ni NN bond length in the lowest energy FM state and the one in the lowest energy NM state [see Fig. 4].

For a given n , we calculate the mean local volume of an iron atom coordinated by a $\text{Fe}_n\text{Ni}_{12-n}$ cluster (V_n) in the NM state. The quantity is approximated as the volume of an iron atom i coordinated by a $\text{Fe}_n\text{Ni}_{12-n}$ cluster; all the pairs formed by the Fe site i and an Fe NN site j are NM. An analogous approach to the one used above is applied to the estimation of V_n in the FM and CF states. Some noteworthy phenomena emerge from the data shown in Fig. 10. (i) While the volume diminishes upon increasing n for the NM alloy, it expands for the FM system. The former effect is due to the fact that d_{ij}^+ [the equilibrium bond length of an Fe-Fe NN pair (i, j)] for the NM configuration is shorter than the distance from atom i to a Ni NN (2.5 Å). Moreover, the latter effect originates from the positive difference between d_{ij}^+ for the FM configuration ($\mathbf{e}_i \cdot \mathbf{e}_j = 1$) and 2.5 Å. (ii) A drop of volume at $n=11$ accompanies the transition from the FM state to the CF state. This is another example of a magnetovolume effect. Indeed, if the exchange energy J_{ij} was independent from the nearest-neighbor distance, then d_{ij}^+ would be equal to 2.435 Å for the FM and AFM arrangements ($\mathbf{e}_i \cdot \mathbf{e}_j = 1$ and $\mathbf{e}_i \cdot \mathbf{e}_j = -1$). Consequently, V_{11} would equal 7.610 Å³ in the FM and CF states.

Besides, Fig. 10 displays the average local volume obtained from *ab initio* calculations versus the local environment parameter in the lowest energy nonmagnetic, ferromagnetic, and collinear ferrimagnetic states. Clearly, the model reproduces the main trends of the first-principles data. Here we would like to note that with increasing n the local arrangement of Fe atoms becomes more similar to fcc Fe. For the highest value of n the average local volume of an Fe atom in the ferromagnetic is larger than those in nonmagnetic and collinear ferrimagnetic states. This agrees with ear-

lier *ab initio* calculations for pure fcc Fe, which showed that the volume of the FM state increased in comparison to the antiferromagnetic and nonmagnetic states, and connected this increase to a transition from Invar to anti-Invar behavior.^{23,42}

V. CONCLUSION

We have carried out a systematic *ab initio* study of static ionic displacements in random $\text{Fe}_{65}\text{Ni}_{35}$ Invar alloy as a function of volume and the alloy magnetic structure. Calculated magnitudes of average Fe-Fe, Fe-Ni, and Ni-Ni $\langle 110 \rangle$ bond vectors have been found to be relatively small, in good agreement with experiment. Regarding distributions of interatomic distances in $\text{Fe}_{65}\text{Ni}_{35}$ at equilibrium, our results indicate that the longest bond is 9% longer than the shortest one. Therefore, individual static displacements can be quite large.

We have focused on an investigation of how fluctuations in the magnetic arrangement affect local geometrical properties of $\text{Fe}_{65}\text{Ni}_{35}$. As far as average Fe-Fe nearest-neighbor bond lengths are concerned, we have found a bigger value in the lowest energy ferromagnetic state than in the lowest energy nonmagnetic state. Furthermore, we have predicted that in the system in a collinear ferrimagnetic state, Fe-Fe nearest-neighbor pairs with moments oriented antiparallel are shorter on average than Fe-Fe first neighbor pairs with parallel moments.

Regarding local volumes of iron atoms in the ferromagnetic alloy, we have observed that (i) for a given n , the volume of an atom coordinated by a $\text{Fe}_n\text{Ni}_{12-n}$ cluster tends to expand upon increasing the local moment at the atom and (ii) the bigger is the number of iron sites in the first coordination shell of a site, the bigger is on average the volume of the atom. Note that the nonmagnetic alloy exhibits a different behavior. Finally, we have observed that the volume associated with an iron site where the moment flips at the FM-CF transition is considerably lowered by the change of magnetic state.

Next, to understand the origin of the effects mentioned above, we have proposed a simple model. The model Hamiltonian has been written as the sum of a chemical energy term and a classical Heisenberg Hamiltonian. We have carefully chosen its input parameters, some of them being *ab initio* results. Examination of structural properties of the model in a NM, FM, and CF states has revealed the existence of behaviors similar to those observed in first-principles calculations. For instance, in a collinear ferrimagnetic state, parallel Fe-Fe NN pairs are longer on average than antiparallel ones. Besides, it has been found that some of the phenomena may be classified as magnetovolume effects, since they arise from an intersite distance dependence of exchange parameters.

ACKNOWLEDGMENTS

The authors are grateful to S. Simak for providing the special quasirandom structure and C. Hooley for reading the manuscript. F.L. wishes to thank G. Ackland, F. Reid, B. Alling, and T. Marten for helping him during his HPC-EUROPA visit at the University of Edinburgh. This

research project was supported by the Swedish Research Council (VR), the European Mineral Sciences Initiative (EuroMinSci) of the European Science Foundation, and the Göran Gustafsson Foundation for Research in Natural Sciences and Medicine. The calculations were carried out at the Swed-

ish Infrastructure for Scientific Computing (SNIC) under the HPC-EUROPA Project No. RII3-CT-2003-506079, with the support of the European Community—Research Infrastructure Action under Grant No. FP6 “Structuring the European Research Area” Programme.

- ¹C. E. Guillaume, *C. R. Acad. Sci.* **125**, 235 (1897).
- ²E. F. Wassermann, in *Ferromagnetic Materials*, edited by K. H. J. Buschow and E. P. Wohlfarth (North-Holland, Amsterdam, 1990), Vol. 5, p. 237.
- ³M. Matsui and S. Chikazumi, *J. Phys. Soc. Jpn.* **45**, 458 (1978).
- ⁴E. I. Kondorsky and V. L. Sedov, *J. Appl. Phys.* **31**, S331 (1960).
- ⁵M. Shiga, *J. Phys. Soc. Jpn.* **22**, 539 (1967).
- ⁶O. Yamada and I. Nakai, *J. Phys. Soc. Jpn.* **50**, 823 (1981).
- ⁷R. J. Weiss, *Proc. Phys. Soc. London* **82**, 281 (1963).
- ⁸W. F. Schlosser, *J. Phys. Chem. Solids* **32**, 939 (1971).
- ⁹U. Krauss and U. Krey, *J. Magn. Magn. Mater.* **98**, L1 (1991).
- ¹⁰A. Zunger, S.-H. Wei, L. G. Ferreira, and J. E. Bernard, *Phys. Rev. Lett.* **65**, 353 (1990).
- ¹¹Z. W. Lu, S.-H. Wei, and A. Zunger, *Phys. Rev. B* **45**, 10314 (1992).
- ¹²P. Olsson, I. A. Abrikosov, and J. Wallenius, *Phys. Rev. B* **73**, 104416 (2006).
- ¹³A. V. Ruban and I. A. Abrikosov, *Rep. Prog. Phys.* **71**, 046501 (2008).
- ¹⁴A. V. Ruban, M. I. Katsnelson, W. Olovsson, S. I. Simak, and I. A. Abrikosov, *Phys. Rev. B* **71**, 054402 (2005).
- ¹⁵A. V. Ruban, S. Khmelevskiy, P. Mohn, and B. Johansson, *Phys. Rev. B* **76**, 014420 (2007).
- ¹⁶I. A. Abrikosov, S. I. Simak, B. Johansson, A. V. Ruban, and H. L. Skriver, *Phys. Rev. B* **56**, 9319 (1997).
- ¹⁷G. Kresse and J. Hafner, *Phys. Rev. B* **48**, 13115 (1993).
- ¹⁸G. Kresse and J. Furthmüller, *Comput. Mater. Sci.* **6**, 15 (1996); *Phys. Rev. B* **54**, 11169 (1996).
- ¹⁹P. E. Blöchl, *Phys. Rev. B* **50**, 17953 (1994).
- ²⁰H. J. Monkhorst and J. D. Pack, *Phys. Rev. B* **13**, 5188 (1976).
- ²¹Y. Wang and J. P. Perdew, *Phys. Rev. B* **44**, 13298 (1991); J. P. Perdew, J. A. Chevary, S. H. Vosko, K. A. Jackson, M. R. Pederson, D. J. Singh, and C. Fiolhais, *ibid.* **46**, 6671 (1992).
- ²²I. A. Abrikosov, A. E. Kissavos, F. Liot, B. Alling, S. I. Simak, O. Peil, and A. V. Ruban, *Phys. Rev. B* **76**, 014434 (2007).
- ²³T. Asada and K. Terakura, *Phys. Rev. B* **46**, 13599 (1992).
- ²⁴T. Hoshino, M. Asato, T. Nakamura, R. Zeller, and P. H. Dederichs, *J. Magn. Magn. Mater.* **272**, E229 (2004).
- ²⁵M. M. Abd-Elmeguid, U. Hobuss, H. Micklitz, B. Huck, and J. Hesse, *Phys. Rev. B* **35**, 4796 (1987).
- ²⁶M. Schröter, H. Ebert, H. Akai, P. Entel, E. Hoffmann, and G. G. Reddy, *Phys. Rev. B* **52**, 188 (1995).
- ²⁷M. van Schilfgaarde, I. A. Abrikosov, and B. Johansson, *Nature (London)* **400**, 46 (1999).
- ²⁸V. Crisan, P. Entel, H. Ebert, H. Akai, D. D. Johnson, and J. B. Staunton, *Phys. Rev. B* **66**, 014416 (2002).
- ²⁹G. Oomi and N. Mori, *J. Phys. Soc. Jpn.* **50**, 2924 (1981).
- ³⁰J. L. Robertson, G. E. Ice, C. J. Sparks, X. Jiang, P. Zschack, F. Bley, S. Lefebvre, and M. Bessiere, *Phys. Rev. Lett.* **82**, 2911 (1999).
- ³¹B. E. Warren, B. L. Averbach, and B. W. Roberts, *J. Appl. Phys.* **22**, 1493 (1951).
- ³²X. Jiang, G. E. Ice, C. J. Sparks, L. Robertson, and P. Zschack, *Phys. Rev. B* **54**, 3211 (1996).
- ³³G. E. Ice, C. J. Sparks, and L. Shaffer, Fall meeting of the Minerals, Metals and Materials Society: Physical Metallurgy and Materials, Pittsburgh, PA, 17–21 October 1993.
- ³⁴M. Acet, H. Zähres, E. F. Wassermann, and W. Pepperhoff, *Phys. Rev. B* **49**, 6012 (1994).
- ³⁵I. Turek and J. Hafner, *Phys. Rev. B* **46**, 247 (1992).
- ³⁶P. Entel, E. Hoffmann, P. Mohn, K. Schwarz, and V. L. Moruzzi, *Phys. Rev. B* **47**, 8706 (1993).
- ³⁷I. A. Abrikosov, O. Eriksson, P. Söderlind, H. L. Skriver, and B. Johansson, *Phys. Rev. B* **51**, 1058 (1995).
- ³⁸D. G. Rancourt and M.-Z. Dang, *Phys. Rev. B* **54**, 12225 (1996).
- ³⁹K. Lagarec, Ph.D. thesis, University of Ottawa, 2001.
- ⁴⁰A. I. Liechtenstein, M. I. Katsnelson, and V. A. Gubanov, *J. Phys. F: Met. Phys.* **14**, L125 (1984).
- ⁴¹A. I. Liechtenstein, M. I. Katsnelson, V. P. Antropov, and V. Gubanov, *J. Magn. Magn. Mater.* **67**, 65 (1987).
- ⁴²H. C. Herper, E. Hoffmann, and P. Entel, *Phys. Rev. B* **60**, 3839 (1999).